From SiO Molecules to Silicates in Circumstellar Space: Atomic Structures, Growth Patterns, and Optical Signatures of Si_nO_m Clusters

Arthur C. Reber,[†] Selvarengan Paranthaman,[†] Peneé A. Clayborne,[†] Shiv N. Khanna,[†,*] and A. Welford Castleman, Jr.[‡]

[†]Department of Physics, Virginia Commonwealth University, Richmond, Virginia 23284, and [‡]Departments of Chemistry and Physics, Pennsylvania State University, University Park, Pennsylvania 16802

ABSTRACT SiO is the dominant silicon bearing molecule in the circumstellar medium; however, it agglomerates to form oxygen-rich silicates. Here we present a synergistic effort combining experiments in beams with theoretical investigations to examine mechanisms for this oxygen enrichment. The oxygen enrichment may proceed *via* two processes, namely, (1) chemically driven compositional separation in $(SiO)_n$ motifs resulting in oxygen-rich and silicon-rich or pure silicon regions, and (2) reaction between Si_nO_m clusters leading to oxygen richer and poorer fragments. While SiO_2 molecules are emitted in selected chemical reactions, they readily oxidize larger Si_nO_n clusters in exothermic reactions and are not likely to agglomerate into larger $(SiO_2)_n$ motifs. Theoretically calculated optical absorption and infrared spectra of Si_nO_m clusters exhibit features observed in the extended red emissions and blue luminescence from interstellar medium, indicating that the Si_nO_m fragments could be contributing to these spectra.

KEYWORDS: silicon oxide clusters · silica formation · interstellar photoluminescence · silicon oxide nanoparticles

Silicates are present throughout circumstellar and interstellar space;[1−5] however, the processes which lead to their formation are poorly understood. Silicates are the main components in young stellar systems and are abundant in interplanetary dust particles.[4,5] The dominant oxygen bearing species in molecular astronomy, which contains both Si and O, is the SiO molecule.[6] Hence it is natural to examine if the silicate formation[7−12] proceeds *via* the clustering of SiO molecules and what possible processes could result in such a formation. Furthermore, what are the atomic structures, stability, and electronic properties of Si_nO_m fragments and what optical signatures could ascertain their presence in interstellar medium? Since the ratio of O to Si in SiO is 1 while it is 2 in SiO_2 and silicates, the clustering of SiO molecules to form silicates has to involve oxygen enrichment.[7] This could occur in a variety of ways.

The clustering of SiO molecules could favor formation of $(SiO)_n$ motifs that have oxygen-poor regions resembling silicon clusters[13−15] and oxygen-rich regions that are like silicates.[9] The origin of this compositional separation is rooted in the chemistry of Si and O atoms. While Si favors tetrahedral bonding, oxygen prefers bonding to one, two, or occasionally three sites,[16,17] leading to regions that satisfy one or the other bonding preference. Indeed, in a recent theoretical study[7] on $(SiO)_n$ clusters containing up to 12 SiO units, we had shown the tendency of Si_nO_n clusters to have oxygen-poor regions and oxygen-rich regions resembling SiO_2 molecules.[15,18−24]

Second, clusters can also undergo fragmentation during growth, into oxygen-poor and oxygen-rich fragments. Some of the pathways involve emission of SiO_2 molecules that can oxidize the larger Si_nO_n or Si_nO_{n+1} species through exothermic reactions. The theoretical findings are supported by laboratory experiments where Si_nO_m clusters are generated starting from a variety of precursors as described in the next section. The formation of silicates can also occur *via* a growth and fragmentation pathway where the energy gained in the reaction of smaller with larger Si_nO_m species can lead to fragmentation into an oxygen richer and poorer fragment.

Finally, the absorption and coalescence between Si_nO_m clusters to form larger species can also lead to emission of an SiO_2 molecule,[7,18,25] and these molecules could assemble to form bulk silicates. However, our studies indicate that the SiO_2 units

*Address correspondence to snkhanna@vcu.edu.

Received for review November 30, 2007 and accepted June 17, 2008.

Published online August 12, 2008.
10.1021/nn7003958 CCC: $40.75

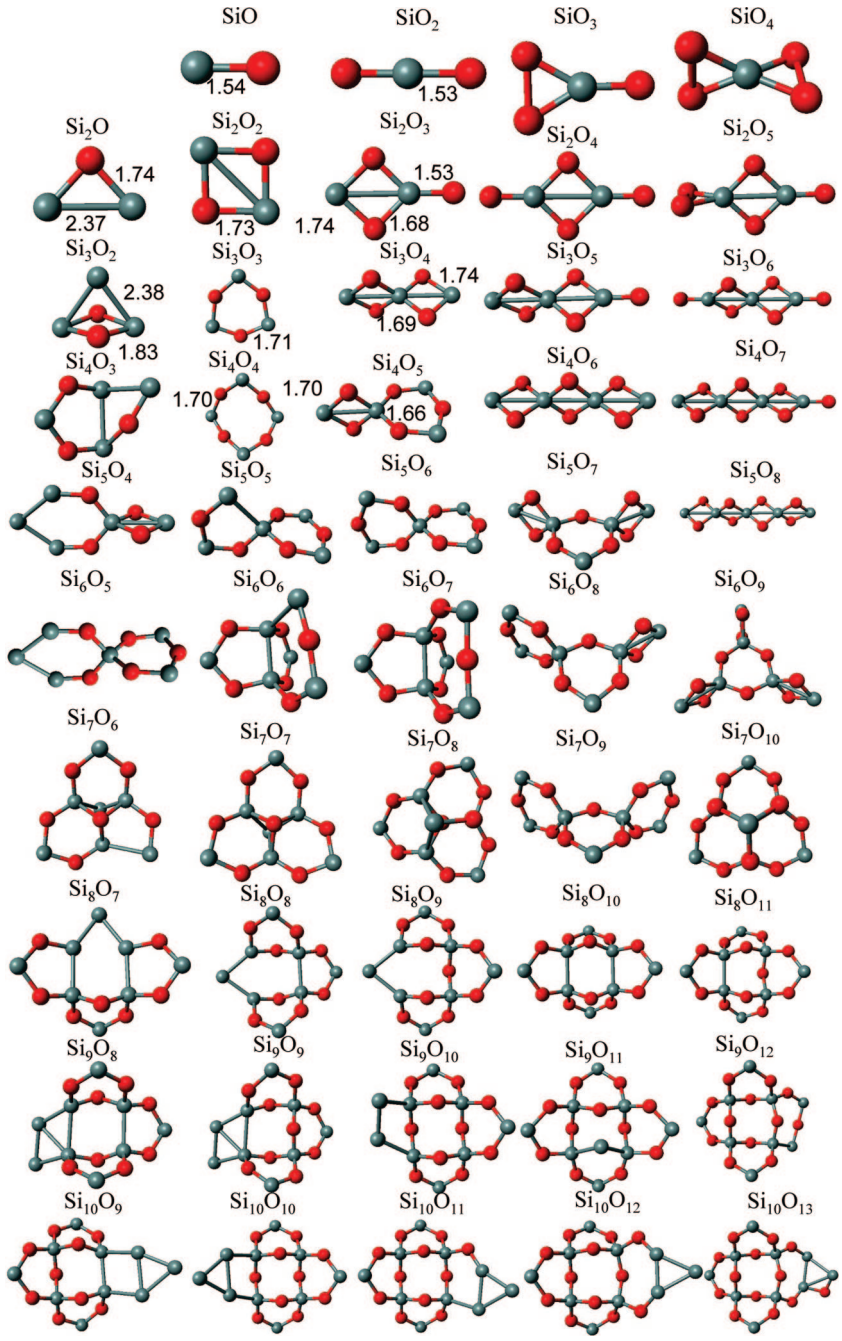

Figure 1. Calculated ground states for Si_nO_m where $n = 1-10$ and $m = n - 1$ through $n + 3$. Gray indicates silicon, red indicates oxygen.

can react with a variety of species and that the direct agglomeration is not the favored mechanism.

These combinations occur in circumstellar and interstellar environments, the feasibility of such processes can only be ascertained through indirect signals. One such signature is the optical spectra.[26] It is then interesting to examine the optical absorption spectra of Si_nO_m species and to explore if the observed spectroscopic features could be associated with the presence of these species. For example, one of the strong signals from spectroscopic measurements is a peak at 2175 Å in the absorption spectrum.[27,28] The origin of this spectral signal and the identity of the motifs responsible for the absorption remain unclear. Could it be due to Si_nO_m clusters?

In this paper, we present the results of a synergistic effort combining laboratory experiments on the clustering of SiO molecules and the first principles theoretical electronic structure studies on $Si_nO_{n\pm x}$ ($-1 \leq x \leq 3$) clusters to examine possible pathways that can contribute to oxygen enrichment as SiO molecules aggregate to form increasingly larger units. The observations in molecular beams are combined with electronic structure studies to present a coherent picture. To make contact with spectroscopic observations, we present theoretical results on the optical absorption spectra of the $Si_nO_{n\pm x}$ clusters and show that the absorption spectra of several clusters are marked by strong features in the vicinity of 2175 Å.[11,27,28] We also calculate the vibrational modes of the clusters and present a first principles study of the infrared (IR) spectrum. In particular, we show that the earlier calculations[29,30] based on parameters derived from the bulk SiO can lead to different values and caution against conclusions based on such calculations. We re-examine the extended red emission and the blue luminescence and show that the majority of clusters have features in the range of 200−700 nm as observed experimentally. Taken together, these results support the presence of Si_nO_m fragments in the interstellar space, thus validating the proposed processes for the formation of silicates.

RESULTS AND DISCUSSION

Formation, Structure, and Electronic Properties of Si_nO_m Clusters: Figure 1 shows the ground-state geometries of Si_nO_{n-1}, Si_nO_n, Si_nO_{n+1}, Si_nO_{n+2}, and Si_nO_{n+3} ($1 \leq n \leq 10$) clusters, while Figure 2 shows the geometries of $Si_nO_{n\pm1}$ ($11 \leq n \leq 16$) clusters. Due to computational restrictions, $n = 16$ was chosen as a maximum size. The corresponding bond lengths are marked in angstroms. There are three bond lengths that mark the structures. The Si−Si bonds range from 2.3 to 2.5 Å, the Si−O bonds in O atoms coordinated to two Si sites range from 1.6 to 1.9 Å, while the Si−O bond lengths where O is bonded to single Si range from 1.5 to 1.6 Å. Our calculations show that a neutral SiO molecule has an atomization energy of 8.30 eV, while the atomization energy of the linear SiO_2 with two SiO bonds is only 13.06 eV with an average energy of 6.53

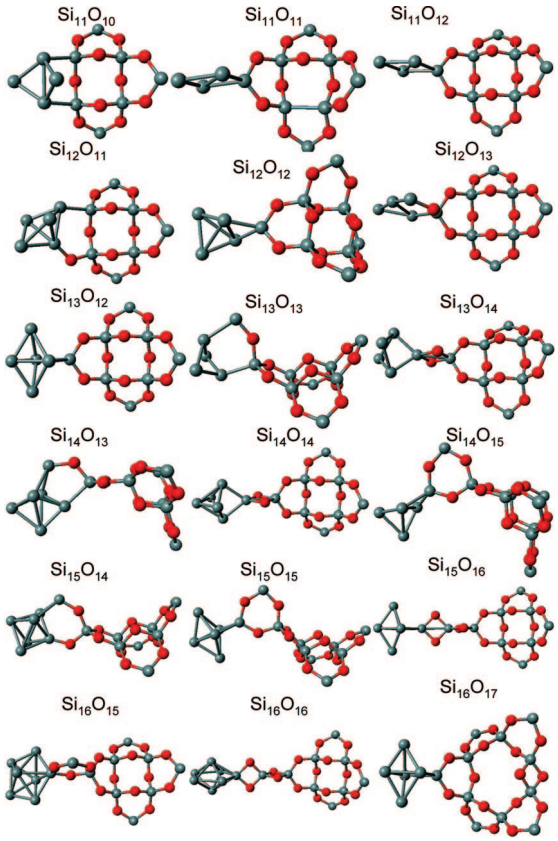

Figure 2. Calculated ground states for Si_nO_m where n = 11−16 and $m = n - 1$ through $n + 1$.

eV per SiO bond. Also, the atomization energy of a Si_2 molecule is 2.45 eV, while that of an O_2 molecule is 5.98 eV. This shows that the SiO bond is the strongest and that, excluding energy barriers, the clusters should prefer to maximize these bonds. This indeed is the case at small sizes where all the Si_nO_m clusters maximize the SiO bonds. In Figure 3, we show the gain in energy as successive SiO units are assembled to form $(SiO)_n$ motifs. Note that Si_3O_3 with a hexagonal ring appears as the first stable species as there is a large gain in energy in forming it from Si_2O_2, whereas the energy gain in growing it to Si_4O_4 is much smaller. The next highly stable species is Si_7O_7 that has three Si_3O_3 rings joined

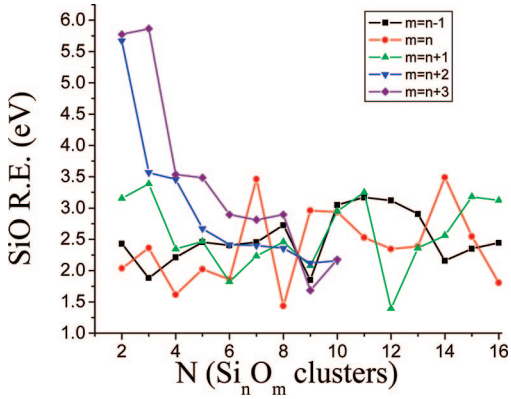

Figure 3. SiO removal energy for Si_nO_m where $m = n - 1$ through $n + 3$.

together with sharing Si and O atoms, and a surprising three-fold coordinated oxygen atom. Similarly, all of the ground-state structures with more than six silicon atoms contain one or more Si_3O_3 rings. In clusters with more than seven silicon atoms, the trend is toward the highly stable Si_8O_{12} motif which is made of four Si_3O_3 rings in a loop.[15] The results also indicate that it takes more than 5.5 eV of energy to remove a SiO from Si_2O_4, Si_2O_5, and Si_3O_6 clusters. In these cases, the drops are not associated with the stability of the parent cluster but rather with the instability of the fragments SiO_3 and Si_2O_5 that are highly oxygen-rich compounds usually have a maximum ratio of 1:2.

One of the key issues relating to the formation of silicates is whether the growth process of SiO molecules can itself lead to formation of silicates. Note that, since SiO bonds are stronger than Si−Si or O−O bonds, the molecular energetics would favor SiO bonds and therefore a more homogeneous distribution of SiO units. On the other hand, as mentioned before, Si and O have very different chemical tendencies. While Si favors tetrahedral coordination, O atoms favor bonding with one, two, or occasionally three atoms.[16,17] This leads to an interesting effect. As the SiO molecules assemble to form larger units, the low coordination of O forces the O atoms to migrate toward one region, resulting in oxygen-rich motifs and silicon-rich regions. The structure of the $Si_{12}O_{12}$ cluster (see Figure 2) is shown to correspond to an oxygen-rich Si_8O_{12} cluster which is reminiscent of a silicate bound to a Si_4 cluster. The present work demonstrates this effect even further by considering larger sizes and a wider composition range. For the Si_nO_n clusters, Figure 1 shows that Si−Si bonds first appear in Si_5O_5 and in Si_7O_7, one of the Si atoms is bonded to two other Si atoms. Further growth results in clusters that have pure silicon regions, SiO-bonded regions, and oxygen-rich regions that can be described as SiO_2 molecules bonded to other atoms. The ratio of Si to O in the mixed region also increases with size. For example, a $Si_{11}O_{11}$ cluster can be looked upon as a Si_3 cluster bound to Si_8O_{11} motif that has a Si to oxygen ratio of 1:1.38. For $Si_{16}O_{16}$ that has a Si_6 bound to $Si_{10}O_{16}$ motif, the Si to O ratio in the oxygen-rich motif increases to 1:1.60. More interestingly, the pure silicon regions are separated from the oxygen-rich region. One also notes that the addition of O to Si_nO_n first results in breaking any Si−Si bonds present in Si_nO_n, and then the formation of SiO_2 units that become linked to Si atoms. As an example, the successive addition of O atoms to Si_5O_5 results in a Si_5O_8 that can be considered as SiO_2 units joined together to form a linear structure. Thus the chemistry of Si and O atoms provides a natural growth pattern resulting in pure Si_n and oxygen-rich regions.

In addition to the chemical processes outlined above, the formation of silicates also proceeds through fragmentation of clusters during the growth process. To illustrate these processes, we start by considering the for-

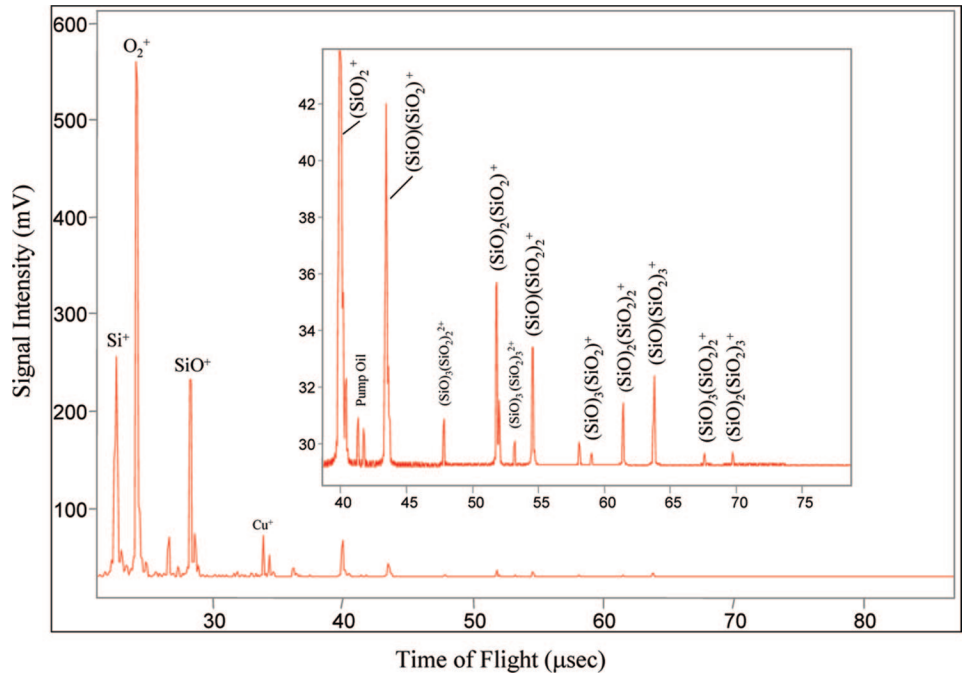

Figure 4. Mass spectrum for silicon laser vaporized under oxygen and helium followed by photoionization of the neutrals.

mation of Si_nO_{n+1} fragments starting from Si_nO_n species. We used our calculated binding energies to examine the possibility of exothermic or nearly isoenergetic processes where Si_nO_n clusters can undergo collision reactions leading to oxygen-enriched fragments. In the following, we list some of these processes along with ΔE in which positive energy indicates exothermic reactions

$$Si_6O_6 + SiO \rightarrow Si_5O_6 + Si_2O \qquad 0.33eV \qquad (1)$$

$$Si_5O_5 + Si_2O_2 \rightarrow Si_5O_6 + Si_2O \qquad 0.16eV \qquad (2)$$

$$Si_6O_6 + Si_2O_2 \rightarrow Si_6O_7 + Si_2O \qquad 0.12eV \qquad (3)$$

In the above, we listed reactions that mostly lead to larger oxygen-rich and smaller oxygen-deficient fragments. We also found processes that result in the emission of SiO_2 molecules and oxygen-deficient larger sizes. In the following, we list some of these processes:

$$Si_6O_6 + Si_6O_6 \rightarrow SiO_2 + Si_{11}O_{10} \qquad 1.29eV \qquad (4)$$

$$Si_4O_4 + Si_8O_8 \rightarrow SiO_2 + Si_{11}O_{10} \qquad 0.27eV \qquad (5)$$

$$Si_8O_8 + Si_5O_5 \rightarrow SiO_2 + Si_{12}O_{11} \qquad 1.37eV \qquad (6)$$

$$Si_2O_3 + Si_6O_6 \rightarrow SiO_2 + Si_7O_7 \qquad 0.31eV \qquad (7)$$

$$Si_2O_3 + Si_2O_3 \rightarrow SiO_2 + Si_3O_4 \qquad 0.23eV \qquad (8)$$

$$Si_6O_7 + Si_{11}O_{12} \rightarrow SiO_2 + Si_{16}O_{17} \qquad 0.41eV \qquad (9)$$

While agglomeration of SiO_2 molecules could, in principle, lead to formation of silicates, we found that SiO_2 are also strong oxidants for larger Si_nO_n clusters. We found several processes where Si_nO_n can react with SiO_2 to generate Si_nO_{n+2} and reactions involving Si_nO_{n+1}, leading to Si_nO_{n+3} species. In the following, we provide a few examples of each of these processes.

Oxygen Enrichment $Si_nO_n \rightarrow Si_mO_{m+2}$

$$Si_4O_4 + SiO_2 \rightarrow Si_3O_5 + Si_2O \qquad 0.15eV \qquad (10)$$

$$Si_4O_4 + SiO_2 \rightarrow Si_4O_6 + Si \qquad 1.32eV \qquad (11)$$

$$Si_5O_5 + SiO_2 \rightarrow Si_3O_5 + Si_3O_2 \qquad 0.05eV \qquad (12)$$

$$Si_5O_5 + SiO_2 \rightarrow Si_4O_6 + Si_2O \qquad 1.58eV \qquad (13)$$

$$Si_5O_5 + SiO_2 \rightarrow Si_5O_7 + Si \qquad 1.83eV \qquad (14)$$

$$Si_6O_6 + SiO_2 \rightarrow Si_3O_5 + Si_4O_3 \qquad 0.37eV \qquad (15)$$

$$Si_6O_6 + SiO_2 \rightarrow Si_4O_6 + Si_3O_2 \qquad 1.61eV \qquad (16)$$

Oxygen Enrichment $Si_nO_{n+1} \rightarrow Si_mO_{m+3}$

$$SiO_2 + Si_5O_6 \rightarrow Si_5O_8 + Si \qquad 0.02eV \qquad (17)$$

$$SiO_2 + Si_6O_7 \rightarrow Si_5O_8 + Si_2O \qquad 0.63eV \qquad (18)$$

$$SiO_2 + Si_7O_8 \rightarrow Si_6O_9 + Si_2O \qquad 1.29eV \qquad (19)$$

We believe that all the above routes lead to the formation of silicates, on the one hand, and small silicon clusters on the other hand.

Experiments were then performed to reveal which clusters are stable enough to coalesce easily as they

exit the plasma source, much as the clusters also must coalesce as they leave the solar envelope. The results were briefly presented in an earlier paper.[7] The experimental studies used a femtosecond laser based time-of-flight mass spectrometer system equipped with a LaVa source.[31,32] The Si_nO_m clusters were generated employing three separate methods. These included vaporization of solid SiO,[33] vaporization of SiO_2, and vaporization of silicon under oxygen. Figure S1 in the Supporting Information is adapted from ref 7 and shows the observed distributions of cations generated through the laser vaporization of SiO solid under an argon environment and subsequently photoionized using 1−2 mJ, 800 nm, 50 fs pulses. For comparison, silicon oxide clusters were also generated by vaporizing silicon under a helium/oxygen environment and analyzing the resulting clusters as described above. The results are shown in Figure 4. In another experiment, cluster cations were extracted directly from the source that are formed in the plasma-like environment existing in the LaVa source which employs a Nd:YAG laser, operated with approximately 4 mJ/pulse photons at 532 nm wavelength. The resulting distribution is shown in Figure 5.

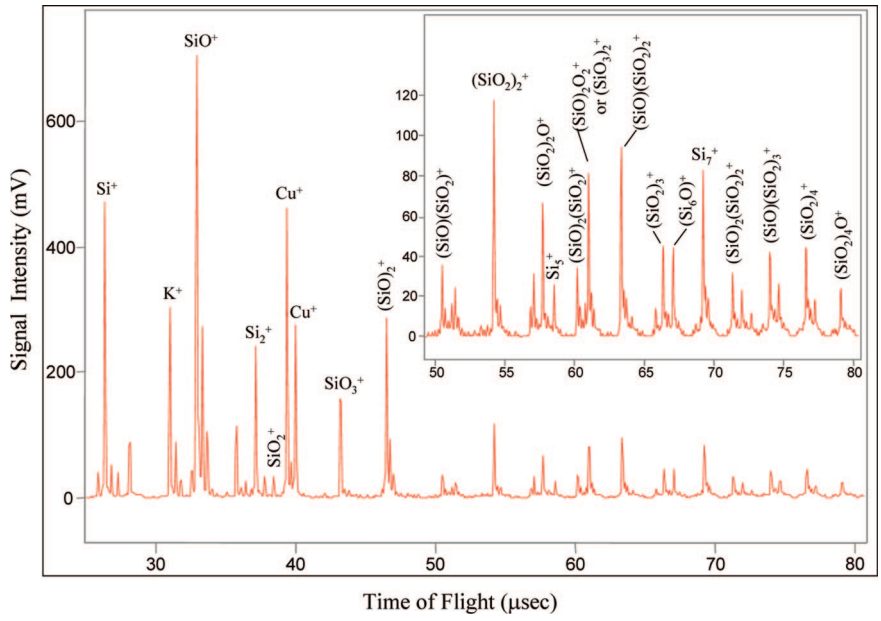

Figure 5. Silicon vaporized under oxygen and helium with cations extracted.

The mass spectra in Figure S1 of the Supporting Information and Figure 4 obtained by ionizing the neutral species formed by vaporizing SiO or silicon under oxygen show that the resulting cations display widely different distributions. However, in all cases including the vaporization of a SiO_2 rod (not shown), $(SiO)_2$ was observed as a major species in the small cluster size distribution and $SiO(SiO_2)$, a stoichiometrically SiO_2 bearing species. However, for the silicon vaporization under O_2/He/cation experiments, the presence of a trace amount of free SiO_2 cation is seen in Figure 5, with a relatively large amount of $(SiO_2)_2$ cation also being produced. The vaporization of SiO and subsequent photoionization of neutrals also gives rise to small pure silicon clusters (Si_n^+, $n = 2-9$), while the vaporization of pure silicon and subsequent oxidation (Figure 4) does not produce any pure silicon species. This can be understood by noting that the SiO bond is stronger than Si−Si and O−O bonds, and hence, if there is sufficient oxygen, the silicon would oxidize rapidly. The presence of significant amounts of SiO^+ in the Si + O_2 spectrum shows that the O−O bond is broken in the LaVa source. The observed species are all oxygen-enriched, showing that pure oxygen is effective at oxidizing the clusters, especially atomic oxygen. Another striking observation is the notable absence of a peak corresponding to SiO_2^+ in either Figure S1 of the Supporting Information or in Figure 4. This is likely due to two reasons. First, as pointed out in our previous paper,[7] SiO_2 has a high ionization potential of 12.18 eV, and hence it is possible that any SiO_2 present in the beam is not ionized. The other reason is that the cation is very reactive. In the following, we list a few of the highly exothermic reactions where a SiO_2^+ can react with other species

$$SiO_2^+ + Si \rightarrow SiO + SiO^+ \quad 4.40eV \qquad (20)$$

$$SiO_2^+ + SiO \rightarrow SiO_2 + SiO^+ \quad 0.85eV \qquad (21)$$

to generate more stable ones. These are probably the reasons that even the vaporization of SiO_2 does not result in any significant amount of cations (see Figure 5). Significantly, $(SiO_2)_2$ cation is formed as a relatively major species in the small-mass range. Its formation may also involve an ion mechanism, as well.

The vaporized SiO and Si under O_2 experimental conditions reveal that SiO agglomeration provides insight into the growth and oxygen enrichment of silicate grains. First of all, note that the vaporized SiO produced significantly more agglomeration than the vaporized Si or SiO_2 experiments, suggesting that SiO or other oxygen carriers may be better suited to produce larger grains than a mixture of Si and O. This is primarily due to SiO_2 addition being so energetic that the etching of the grain is possible, for example, *via* eqs 22 and 23.

$$Si_4O_4 + SiO_2 \rightarrow Si_2O_3 + Si_3O_3 \quad 1.54eV \qquad (22)$$

$$Si_5O_5 + SiO_2 \rightarrow Si_3O_4 + Si_3O_3 \quad 2.90eV \qquad (23)$$

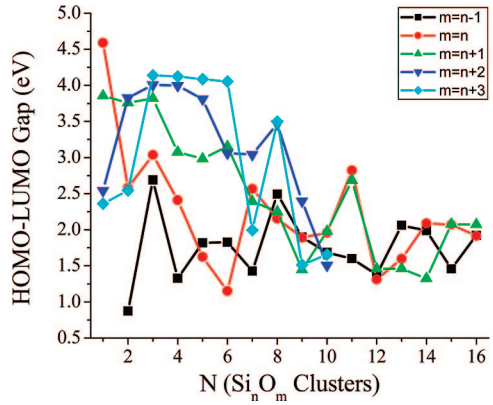

Figure 6. HOMO−LUMO gaps for Si_nO_m clusters $n = 1-10$, $m = (n - 1) - (n + 3)$, and $n = 11-16$, $m = (n - 1) - (n + 1)$.

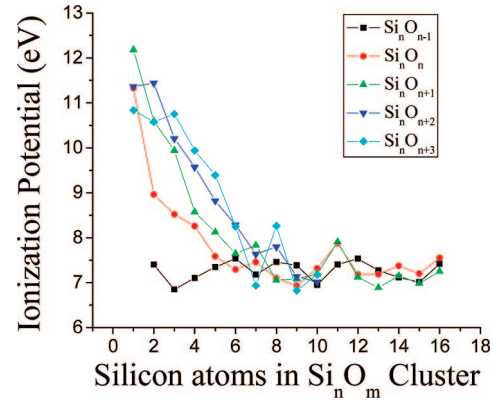

Figure 8. Ionization potential for Si_nO_m clusters $n = 1-16$, $m = (n - 1) - (n + 1)$.

This suggests any observed $(SiO_2)_n$ grains are likely born and grow as $(SiO)_n$ grains and then are oxygen-enriched through a variety of rearrangements involving SiO collisions and oxygen carriers such as SiO_2. The largest observed Si_nO_{n-1} cluster is only Si_3O_2. Si_2O and Si_3O_2 are ubiquitous products in the oxygen enrichment reactions 1−16 because both of these molecules have the maximum number of Si−O bonds while the oxygen removal energy, plotted in Figure S2 of the Supporting Information, increases as the cluster size increases until it flattens out near Si_5O_m and Si_6O_m. Si_4O_7 is the smallest observed $n + 3$ species. It is mass degenerate with Si_8, so there is some uncertainty in the characterization of this peak. These peaks are all consistent with SiO_2 reacting to oxidize rather than forming $(SiO_2)_n$ clusters. To confirm that SiO_2 is indeed present in the experiments, Figure 5 shows the mass spectrum where cations are extracted directly from the plasma, and indeed SiO_2^+ is seen to be present in small concentrations.

We also examined the electronic stability of the various species by calculating the energy gap between the highest occupied molecular orbital (HOMO) and the lowest unoccupied molecular orbital (LUMO), the ionization potential, and the electron affinity of the various species. A large HOMO−LUMO gap is indicative of chemical inertness[34,35] and stability[36] since the cluster wants to neither receive charge nor donate charge. Figure 6 shows the HOMO−LUMO gap, and Si_nO_n clusters with 3, 7, and 11 SiO units have large gaps. The oxygen-rich clusters tend to have larger gaps than silicon-rich species, probably due to the saturation of the Si atoms. Figure 7 shows the calculated electron affinity, and clusters with 2 or 3 Si atoms have low electron affinities. The electron affinities rise with size and are quite large, more than 2 eV for many of the larger clusters. This suggests that the potential that stable anions exist in interstellar medium is possible after the surprising discovery of stable C_6H^- anions in the interstellar medium.[37] It also suggests that these species should bind metals effectively, resulting in the iron- and magnesium-doped silicates. The ionization potentials (IP) of the clusters are shown in Figure 8, and the IP generally decreases with increasing size. Of all the clusters, SiO_2 has the highest ionization potential, namely, 12.18 eV. This is partly the reason that it is not observed upon ionizing neutral species as ionization of SiO_2 would involve multiple photons, and the energy absorbed is sufficient to break the cluster.

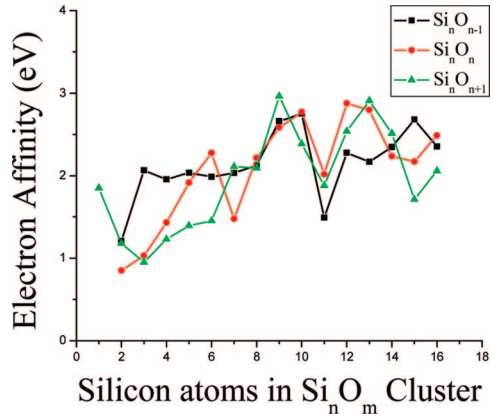

Figure 7. Electron affinity for Si_nO_m clusters $n = 1-16$, $m = (n - 1) - (n + 1)$.

One of the objectives of this paper is to examine if the optical spectra of the Si_nO_m species could account for the feature at 2175 Å[27] and if the vibrational features could account for the observed 10 μm absorption. We first present our findings on the optical properties.

Optical Absorption in Si_nO_m Clusters: Experiments indicated that, while the position of the peak at 2175 Å feature is fairly fixed, its width changes with the line of sight, suggesting that the feature could originate in multiple carriers. In a recent paper, Bradley *et al.* identified this feature to be associated with absorption by polyatomic hydrocarbons and amorphous silicates using transmission electron microscopy.[11] We wanted to examine if the absorption by Si_nO_m clusters could also contribute. While the observed spectrum peaks around 5.7 eV (217.5 nm), it extends to almost 3.0 eV (413.3 nm). We therefore investigated the absorption spectra in the range of 200 to 500 nm.

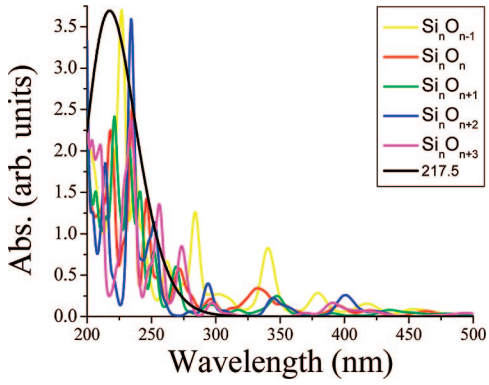

Figure 9. Sum of optical absorptions for all neutral Si_nO_m clusters. The 217.5 nm line is a Gaussian in which $\sigma = 0.5$ eV to guide the eye and approximate the interstellar extinction.

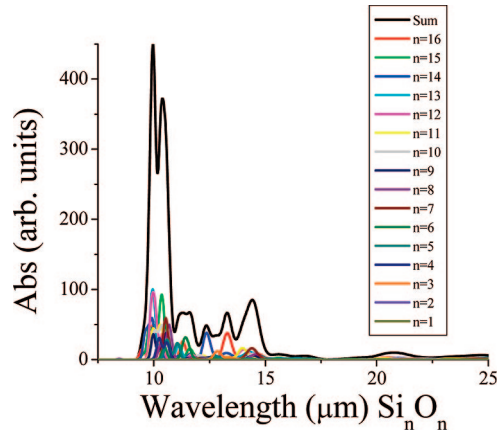

Figure 10. Infrared absorption spectra for Si_nO_n clusters $n = 1-16$.

The theoretical studies covered Si_nO_{n-1}, Si_nO_n, Si_nO_{n+1}, Si_nO_{n+2}, and Si_nO_{n+3} with $1 \leq n \leq 10$ and $Si_nO_{n\pm1}$ clusters with $11 \leq n \leq 16$. We focused in the region of 200−500 nm as the observed spectra fall in this range. Figure 9 and Figures S3−S7 in the Supporting Information present the calculated absorption spectra for Si_nO_{n-1}, Si_nO_n, Si_nO_{n+1}, Si_nO_{n+2}, and Si_nO_{n+3} clusters, respectively. Note that the calculated spectra for most clusters are marked by a peak in the vicinity of 200 nm. To help guide the eye, we have added a Gaussian function centered at 217.5 nm, and with a σ of 0.5 eV, the approximate width of the feature from ref 11. While the location of peaks and the width of the spectra change with size and composition, it is important to note that the majority of spectra have no excitations beyond 400 nm. The location of the common maxima around 200 nm and the absence of absorption features past 400 nm suggest that a superposition of spectra originating in mixed species would produce features close to the observed absorption spectra. To show it more clearly, we present in Figure 9, the spectra obtained by superimposing the calculated spectra shown in Figures S3−S7 in the Supporting Information. Note that the peak position and the width are similar to the observed spectrum. This shows that the Si_nO_m fragments could be contributing to the observed optical absorption.

Infrared Spectra of Si_nO_m Clusters: One of the important tools to identify the constituents of the interstellar dust is infrared spectroscopy. The light from the stars is absorbed by the interstellar dust and re-radiated at infrared wavelengths. Hence the infrared spectrum provides a fingerprint of the emitting clusters.[38] The observed spectra indicate that the interstellar emissions originating in galaxies are dominated by features at 6.2, 7.7, 8.6, and 11.3 μm and are attributed to polyaromatic hydrocarbons.[26,29] The existing models commonly employed to understand these features use spectra calculated for silicate nanoparticles, carbonaceous particles, hydrogenated amorphous carbon, or polyaromatic hydrocarbons. For silicates, the findings are based on the spectrum from bulk crystalline and amorphous silicates that exhibit a resonance around 10 and 20 μm associated with Si−O stretching and O−Si−O bending modes. While amorphous silicates do not exhibit any other peaks, the crystalline silicates also exhibit other resonances beyond 20 μm. The existence of the silicate nanoparticles is then largely based on the comparison of the bulk features or on the infrared spectra for nanoparticles calculated using the bulk parameters in simplified models.

Our objective in this work is to provide an accurate theoretical study of the infrared spectrum of small Si_nO_m clusters using a first principles approach. The primary motivation is to examine if the calculated spectral peaks can be used in conjunction with the observed spectra to demonstrate that the clusters could be contributing to the observed spectra. The present studies also provide opportunities to test the semiempirical models based on bulk parameters. We calculated the spectra for the Si_nO_n clusters for $1 \leq n \leq 16$. Figure 10 shows the calculated spectra for the individual clusters. In each case, we also calculated the combined spectra by superposing the spectra from individual clusters.

Figure 10 shows that, although large Si_nO_n clusters correspond to silicon-rich and SiO_2-rich portions and can be thought of as approaching silicates and silicon clusters, the calculated spectra are very different from the spectra of bulk crystalline and amorphous silicates. For example, the clusters only exhibit a small peak around 20 μm, in contrast to a marked peak shown by the bulk systems. More importantly, the combined spectrum exhibits a marked peak around 11 μm as exhibited by the observed spectra. Further, the calculated transitions are most intense in the region of 10−12 μm. This shows that it is possible that these clusters may possibly be contributing to the observed spectra in addition to the contribution from polyaromatic hydrocarbons. We would like to add that, in this work, we have only considered clusters containing up to 16 SiO

units, and one needs to go to larger sizes to make a more concrete comparison.

CONCLUSIONS

To summarize, our studies provide experiments and first principles information on the atomic and electronic structure, stability, ionization potential, electron affinity, and optical properties of Si_nO_m clusters. We show that the formation of silicates from SiO molecules can proceed either by the chemically driven SiO_2 regions in $(SiO)_n$ motifs or by the sequential oxygen enrichment of Si_nO_m clusters in the coalescence and fragmentation during the growth process. Our studies on the optical absorption exhibit spectral features that lead us to conclude that the Si_nO_m clusters could be contributing to the observed absorption spectra. The calculated infrared spectra indicate that the Si_nO_m particles may be contributing to the observed infrared spectra and also indicate that the existing information on the frequencies of clusters derived from bulk parameters may be erroneous.

EXPERIMENTAL METHODS

The experimental studies were carried out utilizing a femtosecond laser based time-of-flight mass spectrometer system equipped with a laser vaporization (LaVa) source.[30,31] The silicon oxide clusters were generated employing three different methods to examine the nature of the evolving clusters. In one experiment, the clusters were generated by the laser vaporization of SiO solid under an argon environment and photoionized using 1−2 mJ, 800 nm, 50 fs pulses. The product clusters were analyzed using a conventional time-of-flight mass spectrometer. For comparison purposes, other experimental procedures were used including the study of silicon oxide clusters by vaporizing silicon under a helium/oxygen environment and analyzing the resulting clusters as described above and, in other cases, extracting cluster cations directly from the source that are formed in the plasma-like environment existing in the LaVa source which employs a Nd:YAG laser, operated with approximately 4 mJ/pulse photons at 532 nm wavelength. In yet another experiment, the clusters were generated by vaporizing solid SiO_2, whereupon cations were directly extracted. The results of these investigations are used along with theoretical findings to propose a plausible model of silicate formation in circumstellar space.

Theoretical Methods. The theoretical studies are carried out within a density functional theory (DFT),[39] and the exchange correlation contributions are incorporated using the generalized gradient approximation (GGA).[40] The electronic structure was determined by using a linear combination of atomic orbitals molecular orbital approach where the cluster wave function is built out of orbitals centered at the atomic sites. In this work, the atomic orbitals were formed from the triple-ζ valence polarization basis set. The actual calculations were carried out using the deMon code[41] developed by Köster and co-workers. We also used an auxiliary basis set for variational fitting of the Coulomb potential.[42] The numerical integration of the exchange−correlation energy and potential were performed on an adaptive grid.[43] For each size, the geometrical structures were fully optimized in delocalized internal coordinates without constraints using the rational function optimization (RFO) method and the Broyden, Fletcher, Goldfarb, and Shanno (BFGS) update.[44] As Si_nO_m clusters are marked by directional bonds, the local minima are separated by barriers, making the ground-state determination difficult. Consequently, many initial configurations were tried in order to avoid getting trapped in local minima of the potential energy surface.

The calculations on the optical properties were carried out using the Amsterdam Density Functional (ADF)[45] for optical absorption studies, and the molecular structures of the studied species were optimized using gradient-corrected BP86 DFT functional. A triple-ζ with polarization functions (TZP) Slater-type basis set was utilized with a $[1s^2-2p^6]$ frozen core for Si and a $[1s^2]$ frozen core for oxygen atom. The zeroth-order regular approximation (ZORA) was employed in the calculation to account for the scalar relativistic effects.[46] Excited states were calculated using time-dependent DFT (TDDFT).[47] Dipole allowed excitation energies were evaluated for the optical absorption spectrum.

Acknowledgment. A.C.R., S.P., P.A.C., and S.N.K. are grateful to the Department of Energy (DE-FG02−96ER45579), while A.W.C. is grateful to the Air Force Office of Scientific Research (FA9550-07-1-0151) for financial support. We gratefully acknowledge the assistance of S. E. Kooi and B. D. Leskiw in performing the measurements presented in Figures 4, 5, and S1, and Ashraf Ali for bringing this problem area to our attention and participating in acquiring some of the experimental data.

Supporting Information Available: Additional experimental details. This material is available free of charge *via* the Internet at http://pubs.acs.org.

REFERENCES AND NOTES

1. Speck, A. K.; Barlow, M. J.; Sylvester, R. J.; Hofmeister, A. M. Dust Features in the 10-μm Infrared Spectra of Oxygen-Rich Evolved Stars. *Astron. Astrophys. Suppl. Ser.* **2000**, *146*, 437–464.
2. Henning, T. H. In *Solid Interstellar Matter: The ISO Revolution*; D'Hendecourt, L., Joblin, C., Jones, A., Eds.; Springer: Berlin, 1999; pp 247−262.
3. Gordon, K. D.; Witt, A. N.; Friedman, D. G. Detection of Extended Red Emission in the Diffuse Interstellar Medium. *Astrophys. J.* **1998**, *498*, 522–540.
4. Sandford, S. A. The Inventory of Interstellar Materials Available for the Formation of the Solar System. *Meteorit. Planet. Sci.* **1996**, *31*, 449–476.
5. Steel, T. M.; Duley, W. W. A 217.5 Nanometer Absorption Feature in the Spectrum of Small Silicate Particles. *Astrophys. J.* **1987**, *315*, 337–339.
6. Martin-Pintado, J.; Bachiller, R.; Fuente, A. SiO Emission as a Tracer of Shocked Gas in Molecular Outflows. *Astron. Astrophys.* **1992**, *254*, 315–326.
7. Reber, A. C.; Clayborne, P. A.; Reveles, J. U.; Khanna, S. N.; Castleman, A. W., Jr.; Ali, A. Silicon Oxide Nanoparticles Reveal the Origin of Silicate Grains in Circumstellar Environments. *Nano Lett.* **2006**, *6*, 1190–1195.
8. Witt, A. N.; Gordon, K. D.; Furton, D. G. Silicon Nanoparticles: Source of Extended Red Emission. *Astrophys. J.* **1998**, *501*, L111−L115.
9. Nuth, J. A.; Donn, B. Experimental Studies of Vapor Phase Nucleation of Refractory Compounds. II. The Condensation of an Amorphous Magnesium Silicate. *J. Chem. Phys.* **1983**, *78*, 1618–1620.
10. Donn, B.; Nuth, J. A. Does Nucleation Theory Apply to the Formation of Refractory Circumstellar Grains. *Astrophys. J.* **1985**, *288*, 187–190.
11. Bradley, J.; Dai, Z. R.; Erni, R.; Browning, N.; Graham, G.; Weber, P.; Smith, J.; Hutcheon, I.; Ishii, H.; Bajt, S.; et al. An Astronomical 2175 Å Feature in Interplanetary Dust Particles. *Science* **2005**, *307*, 244–247.
12. Gail, H.-P.; Sedlmayr, E. The Primary Condensation Process for Dust Around Late M-Type Stars. *Astron. Astrophys.* **1986**, *166*, 225–236.

13. Zubko, V. G.; Smith, T. L.; Witt, A. N. Silicon Nanoparticles and Interstellar Extinction. *Astrophys. J.* **1999**, *511*, L57–L60.
14. Ho, K. M.; Shvartsburg, A. A.; Pan, B.; Lu, Z. Y.; Wang, C. Z.; Wacker, J. G.; Fye, J. G.; Jarrold, M. F. Structures of Medium-Sized Silicon Clusters. *Nature* **1998**, *392*, 582–585.
15. Wang, H.; Sun, J.; Lu, W. C.; Li, Z. S.; Sun, C. C.; Wang, C. Z.; Ho, K. M. New Motif of Silicon Segregation in Silicon Monoxide Clusters. *J. Phys. Chem. C* **2008**, *112*, 7097–7101.
16. Reber, A. C.; Khanna, S. N.; Hunjan, J. S.; Beltran, M. R. Cobalt Doped Rings and Cages of ZnO Clusters: Motifs for Magnetic Cluster-Assembled Materials. *Chem. Phys. Lett.* **2006**, *428*, 376–380.
17. Reber, A. C.; Khanna, S. N.; Castleman, A. W., Jr. Superatom Compounds and Assemblies: Ultra Alkali Motifs and Architectures. *J. Am. Chem. Soc.* **2007**, *129*, 10189–10194.
18. Marcus, R. A. Mass-Independent Isotope Effect in the Earliest Processed Solids in the Solar System: A Possible Chemical Mechanism. *J. Chem. Phys.* **2004**, *121*, 8201–8211.
19. Bromley, S. T. Thermodynamic Stability of Discrete Fully Coordinated SiO_2 Spherical and Elongated Nanocages. *Nano Lett.* **2004**, *4*, 1427–1432.
20. Nayak, S. K.; Rao, B. K.; Khanna, S. N.; Jena, P. Atomic and Electronic Structure of Neutral and Charged Si_nO_m Clusters. *J. Chem. Phys.* **1998**, *109*, 1245–1250.
21. Chu, T. S.; Zhang, R. Q.; Cheung, H. F. Geometric and Electronic Structures of Silicon Oxide Clusters. *J. Phys. Chem. B* **2001**, *105*, 1705–1709.
22. Zhang, R. Q.; Zhao, M. W.; Lee, S. T. Silicon Monoxide Clusters: The Favorable Precursors for Forming Silicon Nanostructures. *Phys. Rev. Lett.* **2004**, *93*, 095503.
23. Zang, Q. J.; Su, Z. M.; Lu, W. C.; Wang, C. Z.; Ho, K. M. Oxidation Pattern of Small Silicon Oxide Clusters: Structures and Stability of Si_6O_n $n = 1-12$. *J. Phys. Chem. A* **2006**, *110*, 8151–8157.
24. Zang, Q. J.; Su, Z. M.; Lu, W. C.; Wang, C. Z.; Ho, K. M. A First-Principles Study of Oxidation Pattern in Magic Si_7 Clusters. *Chem. Phys. Lett.* **2006**, *430*, 1–7.
25. Ali, A.; Nuth, J. A. The Oxygen Isotope Effect in the Earliest Processed Solids in the Solar System: Is it a Chemical Mass-Independent Process. *Astron. Astrophys.* **2007**, *467*, 919–923.
26. Vijh, U. P. Blue Luminescence and the Presence of Small Polycyclic Aromatic Hydrocarbons in the Interstellar Medium. *Astrophys. J.* **2005**, *633*, 262–271.
27. Stecher, T. P. Interstellar Extinction in the Ultraviolet. II. *Astrophys. J.* **1969**, *157*, L125.
28. Fitzpatrick, E. L. Interstellar Extinction in the Milky Way Galaxy In *Astrophysics of Dust*; Witt, A. N., Clayton, G. C., Draine, B. T., Eds.; ASP Conference Series, 2004, *309*, 33–56.
29. Li, A.; Draine, B. T. Infrared Emission from Interstellar Dust. II. The Diffuse Interstellar Medium. *Astrophys. J.* **2001**, *554*, 778–802.
30. Li, A.; Draine, B. T. Are Silicon Nanoparticles an Interstellar Dust Component. *Astrophys. J.* **2002**, *564*, 803–812.
31. Castleman, A. W., Jr.; Wei, S. Cluster Reactions. *Annu. Rev. Phys. Chem.* **1994**, *45*, 685–719.
32. Kooi, S. E.; Leskiw, B. D.; Castleman, A. W., Jr. Relaxation Dynamics of Electronically Excited Nanoscale Metal-Carbon Complexes: Vanadium-Carbon Clusters. *Nano Lett.* **2001**, *1*, 113–116.
33. Torres, R.; Martin, M. Laser Ablation and Time-of-Flight Mass-Spectrometric Study of SiO. *Appl. Surf. Sci.* **2002**, *193*, 149–155.
34. Pearson, R. G. Absolute Electronegativity and Hardness Correlated with Molecular Orbital Theory. *Proc. Natl. Acad. Sci. U.S.A.* **1986**, *83*, 8440–8441.
35. Reber, A. C.; Khanna, S. N.; Roach, P. J.; Woodward, W. H.; Castleman, A. W., Jr. Spin Accommodation and Reactivity of Aluminum Based Clusters with O_2. *J. Am. Chem. Soc.* **2007**, *129*, 16098–16101.
36. Castleman, A. W., Jr.; Khanna, S. N.; Sen, A.; Reber, A. C.; Qian, M.; Davis, K. M.; Peppernick, S. J.; Ugrinov, A.; Merritt, M. D. From Designer Clusters to Synthetic Crystalline Nanoassemblies. *Nano Lett.* **2007**, *7*, 2734–2741.
37. McCarthy, M. C.; Gottlieb, C. A.; Gupta, H.; and Thaddeus, P. Laboratory and Astronomical Identification of the Negative Molecular Ion C_6H^-. *Astrophys. Lett.* **2006**, *652*, L141–L144.
38. Garand, E.; Goebbert, D.; Santambrogio, G.; Janssens, E.; Lievens, P.; Meijer, G.; Neumark, D. M.; Asmis, K. R. Vibrational Spectra of Small Silicon Monoxide Cluster Cations Measured by Infrared Multiple Photon Dissociation Spectroscopy. *Phys. Chem. Chem. Phys.* **2008**, *10*, 1502–1506.
39. Kohn, R. W.; Sham, L. J. Self Consistent Equations Including Exchange and Correlation Effects. *Phys. Rev.* **1965**, *140*, A1133–A1138.
40. Perdew, J. P.; Burke, K.; Ernzerhof, M. Generalized Gradient Approximation Made Simple. *Phys. Rev. Lett.* **1996**, *77*, 3865–3868.
41. Köster, A. M.; Calaminici, P.; Flores, R.; Geudtner, G.; Goursot, A.; Heine, T.; Janetzko, F.; Patchkovskii, S.; Reveles, J. U.; Vela, A. *deMon*, http://www.deMon-software.com.
42. Köster, A. M.; Reveles, J. U.; del Campo, J. M. Calculation of Exchange-Correlation Potentials with Auxiliary Function Densities. *J. Chem. Phys.* **2004**, *121*, 3417–3424.
43. Köster, A. M.; Flores-Moreno, R.; Reveles, J. U. Efficient and Reliable Numerical Integration of Exchange-Correlation Energies and Potentials. *J. Chem. Phys.* **2004**, *121*, 681–690.
44. Reveles, J. U.; Köster, A. M. Geometry Optimization in Density Functional Methods. *J. Comput. Chem.* **2004**, *25*, 1109–1116.
45. *ADF2006.01d, SCM, Theoretical Chemistry*; Vrije Universiteit: Amsterdam, The Netherlands; http://www.scm.com.
46. Guerra, C. F.; Snijders, J. G.; te Velde, G.; Baerends, E. J. Towards an Order-N DFT Method. *Theor. Chem. Acc.* **1998**, *99*, 391–403.
47. te Velde, G.; Bickelhaupt, F. M.; van Gisbergen, S. J. A.; Guerra, C. F.; Baerends, E. J.; Snijders, J. G.; Ziegler, T. Chemistry with ADF. *J. Comput. Chem.* **2001**, *22*, 931–967.